ELSEVIER

Biophysical Chemistry 125 (2007) 201–212

Biophysical Chemistry

http://www.elsevier.com/locate/biophyschem

A mesoscopic stochastic mechanism of cytosolic calcium oscillations

Chun-lian Zhu [a,b], Ya Jia [b,*], Quan Liu [b], Li-jian Yang [b], Xuan Zhan [b]

[a] *Department of Physics, Jianghan University, Wuhan 430056, China*
[b] *School of Physics and Institute of Biophysics, Central China Normal University, Wuhan 430079, China*

Received 29 April 2006; received in revised form 1 August 2006; accepted 2 August 2006
Available online 15 August 2006

Abstract

Based on a model of intracellular calcium (Ca^{2+}) oscillation with self-modulation of inositol 1,4,5-trisphosphate signal, the mesoscopic stochastic differential equations for the intracellular Ca^{2+} oscillations are theoretically derived by using the chemical Langevin equation method. The effects of the finite biochemical reaction molecule number on both simple and complex cytosolic Ca^{2+} oscillations are numerically studied. In the case of simple intracellular Ca^{2+} oscillation, it is found that, with the increase of molecule number, the coherence resonance or autonomous resonance phenomena can occur for some external stimulation parameter values. In the cases of complex cytosolic Ca^{2+} oscillations, each extremum of concentration of cytosolic Ca^{2+} oscillations corresponds to a peak in the histogram of Ca^{2+} concentration, and the most probability appeared during the bursting plateau level for bursting, but at the largest minimum of Ca^{2+} concentration for chaos. For quasi-periodicity, however, there are only two peaks in the histogram of Ca^{2+} concentration, and the most probability is located at low concentration state.

Keywords: Intracellular calcium oscillations; Chemical Langevin equation; Finite molecule number

1. Introduction

Calcium (Ca^{2+}) is one of the most important messengers in the cytosol of living cells. Intracellular Ca^{2+} oscillations play a significant role in signal transduction from receptors at the cell membrane to enzymes and genes controlling the complex biochemical network of cell [1–22]. The information in Ca^{2+} oscillations can be encoded by their frequency [16–20] as well as by their amplitude [21–23].

Intracellular calcium dynamics has been intensively studied in different theoretical models (for comprehensive reviews see Schuster et al. [24] and Falcke [25]). In the deterministic approach, various models with the macroscopic differential equations have been developed for the widespread phenomenon in intra- and intercellular Ca^{2+} oscillating signalling, much insight has been gained into the processes involved in Ca^{2+} dynamics at the subcellular, cellular and intercellular levels, and the models of calcium oscillations have become more elaborate and diversified [24–55]. In particular, various oscillating behaviors (e.g. bursting, chaos, and quasi-periodicity), different types of bifurcations, and the coupling between oscillating cells have been analyzed. There are many more models and ways to generate complex intracellular Ca^{2+} oscillations [24,25]. Complex Ca^{2+} oscillations may arise through the interplay between two oscillatory mechanisms, but this is not the only possibility, for instance, different agonists may induce different oscillating types in the same cell type [54].

In realistic biological system, however, various internal and external fluctuations cannot be negligible. For the internal fluctuations, one source of fluctuations in intracellular Ca^{2+} concentration arises from random releasing of Ca^{2+} channels embedded in the membrane of intracellular stores like the endoplasmic reticulum (ER) [25,58,60]. Thus, some stochastic models have been developed for single Ca^{2+} channels [57], cluster of IP_3R channels [58,60–63], intracellular wave propagation [59,64–68] and intracellular oscillations [69,70]. On the other hand, the cellular biochemical reactions usually occurred in finite system, or the total numbers of biochemical reaction molecules in cell are often finite. At a given temperature, the occurrence of each biochemical reaction

* Corresponding author.
E-mail address: jiay@phy.ccnu.edu.cn (Y. Jia).

0301-4622/$ - see front matter © 2006 Elsevier B.V. All rights reserved.
doi:10.1016/j.bpc.2006.08.001

event in cellular systems is random due to thermal agitation, which is another source of intrinsic fluctuations in intracellular Ca^{2+} oscillations. Furthermore, this intrinsic fluctuation is self-originated in the system. An important fact about the internal fluctuation is that it scales with the system size, and vanishes in the thermodynamic limit. Therefore, for a typical living cell system, the macroscopic differential equations description to intracellular Ca^{2+} oscillations is no longer valid due to the finite size of system, one should consider the effects of finite biochemical reaction molecule number on the intracellular Ca^{2+} oscillations, and a mesoscopic stochastic kinetics should be offered to describe the mechanism of intracellular calcium oscillations. Recently, there has been an increasing interest in the finite size effects on some biological systems [57,71–74].

Now a question to be raised is how to describe the mesoscopic mechanism of intracellular Ca^{2+} oscillations in finite cellular volume, or what are the effects of finite biochemical reaction molecule number on the intracellular Ca^{2+} oscillations. In the present paper, as an example, the deterministic model of intracellular Ca^{2+} oscillation with self-modulation of IP_3 signal proposed by Houart et al. [46] to describe both simple and complex intracellular calcium oscillations has been chosen here. It should be stressed that, to obtain complex Ca^{2+} oscillations, the stochastic models do not require feedback of Ca^{2+} on IP_3 [25,58], for instance, the external noise-induced bursting in a two-variable cytosolic Ca^{2+} oscillation model [56].

The mesoscopic stochastic differential equations for this model have been theoretically derived by using the chemical Langevin equation (CLE) [75] in Section 2. In Section 3, the effects of internal fluctuation due to the finite biochemical reaction molecule number in cell on both simple and complex intracellular Ca^{2+} oscillations have been theoretically studied through numerical computation, respectively. In the case of simple intracellular Ca^{2+} oscillation, it is found that there might be a large signal-to-noise ratio (SNR) with the increase of total molecule number for some external stimulation parameter values, which corresponds to the coherence resonance or autonomous resonance phenomena. In the case of complex intracellular Ca^{2+} oscillations, the histograms of cytosolic Ca^{2+} concentration are different for each typical complex Ca^{2+} oscillatory behavior in finite biochemical reaction molecule number. Finally, we end with conclusions in Section 4.

2. Mesoscopic stochastic differential equations for intracellular Ca^{2+} oscillations

The key species in the model of intracellular Ca^{2+} oscillation with self-modulation of IP_3 signal [46] are the cytosolic Ca^{2+} (its concentration is represented by Z), the Ca^{2+} sequester in an internal store (its concentration is represented by Y), and the IP_3 (its concentration is represented by A) which is another important intracellular messenger. The time evolution of these species can be described by following macroscopic differential equations

$$\frac{dZ}{dt} = V_0 + V_1\beta - V_2 + V_3 + k_f Y - kZ, \tag{1}$$

$$\frac{dY}{dt} = V_2 - V_3 - k_f Y, \tag{2}$$

$$\frac{dA}{dt} = \beta V_4 - V_5 - \varepsilon A, \tag{3}$$

where the external stimulation parameter β reflects the degree of stimulation of the cell by an agonist and thus only varies between 0 and 1, and has two Hopf bifurcation points. Detail description of other parameters in this model can be found in Table 1.

The three species S_i ($i=1, 2, 3$) considered here are cytosolic Ca^{2+}, Ca^{2+} sequester in internal store, and intracellular IP_3, respectively. It is introduced that the number of calcium ions in cytosol as z, the number of calcium ions in internal store as y, and the number of IP_3 molecules in cytosol as a. Then, the relationship between the concentration and the total number of molecules is

$$Z = \frac{z}{\Omega}, \quad Y = \frac{y}{\Omega}, \quad A = \frac{a}{\Omega}, \tag{4}$$

where Ω is defined as the total molecule (including the cytosolic Ca^{2+}, intravesicular Ca^{2+}, and intracellular IP_3) number in cell. Nine elementary biochemical reaction processes are considered in the model of intracellular Ca^{2+} oscillation with self-modulation of IP_3 signal. Note that there are twelve reaction channels R_j ($j=1,\ldots, 12$) for the three species S_i ($i=1, 2, 3$) as shown in Fig. 1, where the reaction channels R_3 and R_7, R_4 and R_8, and R_5 and R_9 represent the same biochemical reaction process, respectively. The transition rates of the twelve reaction channels are marked by $r_j=1,\ldots, 12$. The corresponding transition rates for the twelve channels are described in Table 2, where the transition rates are proportional to the total number of intracellular molecules Ω. The transition rate r_j for R_j and the state-change vector $\overrightarrow{v_j}$, whose ith component $v_{j,i}$ is the change in

Table 1
Parameters in the model of intracellular Ca^{2+} oscillations [46]

Parameter	Description
V_0	Constant input from extracellular medium
V_1	Maximum rate of stimulus-induced influx from the extracellular medium
V_2	Pump flux of cytosolic Ca^{2+} into the internal stores with a maximum value V_{M2}, $V_2 = V_{M2}\frac{Z^2}{K_2^2+Z^2}$
V_3	Release of Ca^{2+} from internal stores with a maximum value V_{M3}, $V_3 = V_{M3}\frac{Z^m}{K_Z^m+Z^m}\frac{Y^2}{K_Y^2+Y^2}\frac{A^4}{K_A^4+A^4}$
V_4	Maximum rate of stimulus-induced synthesis of IP_3
V_5	Rate of phosphorylation of IP_3 by the 3-kinase with a maximum value V_{M5} and a half-saturation constant K_5, $V_5 = V_{M5}\frac{A^p}{K_5^p+A^p}\frac{Z^n}{K_d^n+Z^n}$
K_2	Threshold constant for pumping
K_Y	Threshold constant for release by Ca^{2+}
K_Z	Threshold constant for activation by Ca^{2+}
K_A	Threshold constant for activation by IP_3
k_f	Rate constant measuring the passive, linear leak of Y into Z
k	Rate constant of linear transport of cytosolic Ca^{2+} into the extracellular medium
K_d	Threshold constant for 3-kinase stimulated by Ca^{2+}

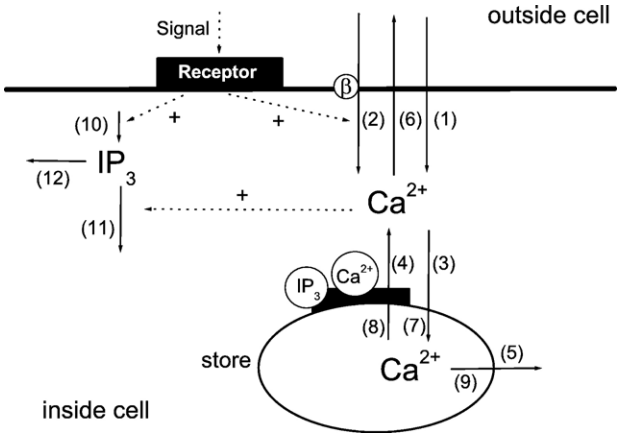

Fig. 1. The schematic description of the model [46]. There are twelve reaction channels marked with (1)–(12), respectively.

the number of S_i (i=1, 2, 3) molecules produced by one R_j (j=1, …, 12) reaction channel, together completely specify the reaction channel R_j.

Table 2
Reaction channels and corresponding transition rates

Reaction channels	Description	Transition rates
(1) $z\to z+1$	Constant input of cytosolic Ca^{2+} from extracellular medium	$r_1=\Omega V_0$
(2) $z\to z+1$	Stimulus-induced influx of cytosolic Ca^{2+} from extracellular medium	$r_2=\Omega V_1\beta$
(3) $z\to z-1$	Pumping of cytosolic Ca^{2+} into internal store	$r_3=\Omega\frac{V_{M2}Z^2}{K_Z^2+Z^2}$
(4) $z\to z+1$	Input of cytosolic Ca^{2+} from internal store	$r_4=\Omega\frac{V_{M3}Z^m}{K_Z^m+Z^m}\frac{Y^2}{K_Y^2+Y^2}\frac{A^4}{K_A^4+A^4}$
(5) $z\to z+1$	Input of cytosolic Ca^{2+} from internal store	$r_5=\Omega k_f Y$
(6) $z\to z-1$	Leakage of cytosolic Ca^{2+} into extracellular medium	$r_6=\Omega kZ$
(7) $y\to y+1$	Pumping of cytosolic Ca^{2+} into internal store	$r_7=\Omega\frac{V_{M2}Z^2}{K_2^2+Z^2}$
(8) $y\to y-1$	Release of Ca^{2+} from internal store	$r_8=\Omega\frac{V_{M3}Z^m}{K_Z^m+Z^m}\frac{Y^2}{K_Y^2+Y^2}\frac{A^4}{K_A^4+A^4}$
(9) $y\to y-1$	Leakage of internal pool Ca^{2+} from internal store	$r_9=\Omega k_f Y$
(10) $a\to a+1$	Stimulus-induced synthesis of IP_3	$r_{10}=\Omega\beta V_4$
(11) $a\to a-1$	Phosphorylated IP_3 by 3-kinase	$r_{11}=\Omega\frac{V_{M5}A^P}{K_5^P+A^P}\frac{Z^n}{K_d^n+Z^n}$
(12) $a\to a-1$	Metabolized IP_3 by 5-phosphatase	$r_{12}=\Omega\epsilon A$

Following along the Gillespie's method [75], suppose the system's state at the current time t is known to be ($z(t)$, $y(t)$, $a(t)$). Let a random variable $K_j(z(t), y(t), a(t), \tau)$, for any $\tau>0$, be the number of R_j reactions that occur in the subsequent time interval $[t, t+\tau]$. Since each of those reactions will increase the S_i population by $v_{j,i}$ (see Table 3), thus, the number of S_i molecules in the system at time $t+\tau$ will be

$$\begin{aligned} z(t+\tau) = z(t) &+ K_1(z(t),y(t),a(t),\tau) \\ &+ K_2(z(t),y(t),a(t),\tau) - K_3(z(t),y(t),a(t),\tau) \\ &+ K_4(z(t),y(t),a(t),\tau) + K_5(z(t),y(t),a(t),\tau) \\ &- K_6(z(t),y(t),a(t),\tau), \end{aligned} \quad (5)$$

$$\begin{aligned} y(t+\tau) = y(t) &+ K_7(z(t),y(t),a(t),\tau) \\ &- K_8(z(t),y(t),a(t),\tau) - K_9(z(t),y(t),a(t),\tau), \end{aligned} \quad (6)$$

$$\begin{aligned} a(t+\tau) = a(t) &+ K_{10}(z(t),y(t),a(t),\tau) \\ &- K_{11}(z(t),y(t),a(t),\tau) - K_{12}(z(t),y(t),a(t),\tau). \end{aligned} \quad (7)$$

An excellent approximation to $K_j(z(t), y(t), a(t), \tau)$ in Eqs. (5)–(7) can be obtained if the following two conditions are imposed [75]. (i) Require τ to be small enough that the change in the state during $[t, t+\tau]$ will be so slight that none of the propensity functions changes its value appreciably. Each $K_j(z(t), y(t), a(t), \tau)$ will be a statistically independent Poisson random variable, $\mathcal{P}_j(r_j(z(t), y(t), a(t)), \tau)$. Eqs. (5)–(7) are approximated by

$$\begin{aligned} z(t+\tau) = z(t) &+ \mathcal{P}_1(r_1(z(t),y(t),a(t)),\tau) \\ &+ \mathcal{P}_2(r_2(z(t),y(t),a(t)),\tau) - \mathcal{P}_3(r_3(z(t),y(t),a(t)),\tau) \\ &+ \mathcal{P}_4(r_4(z(t),y(t),a(t)),\tau) + \mathcal{P}_5(r_5(z(t),y(t),a(t)),\tau) \\ &- \mathcal{P}_6(r_6(z(t),y(t),a(t)),\tau), \end{aligned} \quad (8)$$

$$\begin{aligned} y(t+\tau) = y(t) &+ \mathcal{P}_7(r_7(z(t),y(t),a(t)),\tau) \\ &- \mathcal{P}_8(r_8(z(t),y(t),a(t)),\tau) - \mathcal{P}_9(r_9(z(t),y(t),a(t)),\tau), \end{aligned} \quad (9)$$

$$\begin{aligned} a(t+\tau) = a(t) &+ \mathcal{P}_{10}(r_{10}(z(t),y(t),a(t)),\tau) \\ &- \mathcal{P}_{11}(r_{11}(z(t),y(t),a(t)),\tau) \\ &- \mathcal{P}_{12}(r_{12}(z(t),y(t),a(t)),\tau). \end{aligned} \quad (10)$$

(ii) Require τ to be large enough that the expected number of occurrences of each reaction channel R_j in $[t, t+\tau]$ be much larger than 1, which allows us to approximate each Poisson random variable $\mathcal{P}_j(r_j(z(t), y(t), a(t)), \tau)$ by a normal random variable with

Table 3
Population change $v_{j,i}$ of specie S_i (i=1, 2, 3) in R_j (j=1, …, 12) reaction channel

Specie	Population change
S_1 (cytosolic Ca^{2+})	$v_{1,1}=v_{2,1}=1$, $v_{3,1}=-1$, $v_{4,1}=v_{5,1}=1$, $v_{6,1}=-1$, $v_{7,1}=v_{8,1}=v_{9,1}=v_{10,1}=v_{11,1}=v_{12,1}=0$
S_2 (Ca^{2+} in internal store)	$v_{1,2}=v_{2,2}=v_{3,2}=v_{4,2}=v_{5,2}=v_{6,2}=0$, $v_{7,2}=1$, $v_{8,2}=v_{9,2}=-1$, $v_{10,2}=v_{11,2}=v_{12,2}=0$
S_3 (intracellular IP_3)	$v_{1,3}=v_{2,3}=v_{3,3}=v_{4,3}=v_{5,3}=v_{6,3}=v_{7,3}=v_{8,3}=v_{9,3}=0$, $v_{10,3}=1$, $v_{11,3}=v_{12,3}=-1$

the same mean and variance. That brings Eqs. (8)–(11) into the form

$$\begin{aligned} z(t+\tau) = z(t) &+\mathcal{N}_1(r_1(z(t),y(t),a(t))\tau, r_1(z(t),y(t),a(t))\tau) \\ &+\mathcal{N}_2(r_2(z(t),y(t),a(t))\tau, r_2(z(t),y(t),a(t))\tau) \\ &-\mathcal{N}_3(r_3(z(t),y(t),a(t))\tau, r_3(z(t),y(t),a(t))\tau) \\ &+\mathcal{N}_4(r_4(z(t),y(t),a(t))\tau, r_4(z(t),y(t),a(t))\tau) \\ &+\mathcal{N}_5(r_5(z(t),y(t),a(t))\tau, r_5(z(t),y(t),a(t))\tau) \\ &-\mathcal{N}_6(r_6(z(t),y(t),a(t))\tau, r_6(z(t),y(t),a(t))\tau), \end{aligned} \quad (11)$$

$$\begin{aligned} y(t+\tau) = y(t) &+\mathcal{N}_7(r_7(z(t),y(t),a(t))\tau, r_7(z(t),y(t),a(t))\tau) \\ &-\mathcal{N}_8(r_8(z(t),y(t),a(t))\tau, r_8(z(t),y(t),a(t))\tau) \\ &-\mathcal{N}_9(r_9(z(t),y(t),a(t))\tau, r_9(z(t),y(t),a(t))\tau), \end{aligned} \quad (12)$$

$$\begin{aligned} a(t+\tau) = a(t) &+\mathcal{N}_{10}(r_{10}(z(t),y(t),a(t))\tau, r_{10}(z(t),y(t),a(t))\tau) \\ &-\mathcal{N}_{11}(r_{11}(z(t),y(t),a(t))\tau, r_{11}(z(t),y(t),a(t))\tau) \\ &-\mathcal{N}_{12}(r_{12}(z(t),y(t),a(t))\tau, r_{12}(z(t),y(t),a(t))\tau), \end{aligned} \quad (13)$$

where $N_j(m_j,\sigma_j^2)$ denotes the normal random variable with mean m_j and variance σ_j^2, and is statically independent with each other because of the statistically independent Poisson random variable. The molecular populations from discretely changing integer variables in Eqs. (8)–(10) are converted to continuously changing real variables in Eqs. (11)–(13) in effect. The linear combination theorem for normal random variables,

$$\mathcal{N}_j(m_j,\sigma_j^2) = m_j + \sigma_j\mathcal{N}_j(0,1), \quad (14)$$

can now be invoked to bring Eqs. (11)–(13) into the form

$$\begin{aligned} z(t+\tau) = z(t) &+ r_1(z(t),y(t),a(t))\tau \\ &+r_2(z(t),y(t),a(t))\tau - r_3(z(t),y(t),a(t))\tau \\ &+r_4(z(t),y(t),a(t))\tau) + r_5(z(t),y(t),a(t))\tau) \\ &-r_6(z(t),y(t),a(t))\tau \\ &+[r_1(z(t),y(t),a(t))\tau]^{1/2}\mathcal{N}_1(0,1) \\ &+[r_2(z(t),y(t),a(t))\tau]^{1/2}\mathcal{N}_2(0,1) \\ &-[r_3(z(t),y(t),a(t))\tau]^{1/2}\mathcal{N}_3(0,1) \\ &+[r_4(z(t),y(t),a(t))\tau]^{1/2}\mathcal{N}_4(0,1) \\ &+[r_5(z(t),y(t),a(t))\tau]^{1/2}\mathcal{N}_5(0,1) \\ &-[r_6(z(t),y(t),a(t))\tau]^{1/2}\mathcal{N}_6(0,1) \end{aligned} \quad (15)$$

$$\begin{aligned} y(t+\tau) = y(t) &+ r_7(z(t),y(t),a(t))\tau \\ &-r_8(z(t),y(t),a(t))\tau - r_9(z(t),yt,a(t))\tau \\ &+[r_7(z(t),y(t),a(t))\tau]^{1/2}\mathcal{N}_7(0,1) \\ &-[r_8(z(t),y(t),a(t))\tau]^{1/2}\mathcal{N}_8(0,1) \\ &-[r_9(z(t),y(t),a(t))\tau]^{1/2}\mathcal{N}_9(0,1), \end{aligned} \quad (16)$$

$$\begin{aligned} a(t+\tau) = a(t) &+ r_{10}(z(t),y(t),a(t))\tau \\ &-r_{11}(z(t),y(t),a(t))\tau - r_{12}(z(t),y(t),a(t))\tau \\ &+[r_{10}(z(t),y(t),a(t))\tau]^{1/2}\mathcal{N}_{10}(0,1) \\ &-[r_{11}(z(t),y(t),a(t))\tau]^{1/2}\mathcal{N}_{11}(0,1) \\ &+[r_{12}(z(t),y(t),a(t))\tau]^{1/2}\mathcal{N}_{12}(0,1), \end{aligned} \quad (17)$$

where $N_{j=1,\ldots,12}(0,1)$ are statically independent with each other. Let us regard any time interval τ that satisfies both conditions (i) and (ii) as a macroscopic infinitesimal, and denote it simply by dt, and write the unit normal random variable $N_j(0,1)$ as $N_j(t)$. Eqs. (15)–(17) become

$$\begin{aligned} z(t+\mathrm{dt}) = z(t) &+ r_1(z(t),y(t),a(t))\mathrm{dt} \\ &+r_2(z(t),y(t),a(t))\mathrm{dt} - r_3(z(t),y(t),a(t))\mathrm{dt} \\ &+r_4(z(t),y(t),a(t))\mathrm{dt} + r_5(z(t),y(t),a(t))\mathrm{dt} \\ &-r_6(z(t),y(t),a(t))\mathrm{dt} \\ &+r_1^{1/2}(z(t),y(t),a(t))\mathcal{N}_1(t)(\mathrm{dt})^{1/2} \\ &+r_2^{1/2}(z(t),y(t),a(t))\mathcal{N}_2(t)(\mathrm{dt})^{1/2} \\ &-r_3^{1/2}(z(t),y(t),a(t))\mathcal{N}_3(t)(\mathrm{dt})^{1/2} \\ &+r_4^{1/2}(z(t),y(t),a(t))\mathcal{N}_4(t)(\mathrm{dt})^{1/2} \\ &+r_5^{1/2}(z(t),y(t),a(t))\mathcal{N}_5(t)(\mathrm{dt})^{1/2} \\ &-r_6^{1/2}(z(t),y(t),a(t))\mathcal{N}_6(t)(\mathrm{dt})^{1/2}, \end{aligned} \quad (18)$$

$$\begin{aligned} y(t+\mathrm{dt}) = y(t) &+ r_7(z(t),y(t),a(t)),\mathrm{dt} \\ &-r_8(z(t),y(t),a(t))\mathrm{dt} - r_9(z(t),y(t),a(t))\mathrm{dt} \\ &+r_7^{1/2}(z(t),y(t),a(t)\mathcal{N}_7(t)(\mathrm{dt})^{1/2} \\ &-r_8^{1/2}(z(t),y(t),a(t))\mathcal{N}_8(t)(\mathrm{dt})^{1/2} \\ &-r_9^{1/2}(z(t),y(t),a(t))\mathcal{N}_9(t)(\mathrm{dt})^{1/2}, \end{aligned} \quad (19)$$

$$\begin{aligned} a(t+\mathrm{dt}) = a(t) &+ r_{10}(z(t),y(t),a(t))\mathrm{dt} \\ &-r_{11}(z(t),y(t),a(t))\mathrm{dt} - r_{12}(z(t),y(t),a(t))\mathrm{dt} \\ &+r_{10}^{1/2}(z(t),y(t),a(t))\mathcal{N}_{10}(t)(\mathrm{dt})^{1/2} \\ &-r_{11}^{1/2}(z(t),y(t),a(t))\mathcal{N}_{11}(t)(\mathrm{dt})^{1/2} \\ &-r_{12}^{1/2}(z(t),y(t),a(t))\mathcal{N}_{12}(t)(\mathrm{dt})^{1/2}. \end{aligned} \quad (20)$$

Eqs. (18)–(20) have the canonical form of standard Langevin equations for multivariate continuous Markov processes. Thus, Eqs. (18)–(20) imply the equivalent white-noise form Langevin equation

$$\begin{aligned} \frac{\mathrm{d}z(t)}{\mathrm{d}t} = r_1(z(t),y(t),a(t)) &+ r_2(z(t),y(t),a(t)) \\ &-r_3(z(t),y(t),a(t)) + r_4(z(t),y(t),a(t)) \\ &+r_5(z(t),y(t),a(t)) - r_6(z(t),y(t),a(t)) \\ &+r_1^{1/2}(z(t),y(t),a(t))\xi_1(t) \\ &+r_2^{1/2}(z(t),y(t),a(t))\xi_2(t) \\ &-r_3^{1/2}(z(t),y(t),a(t))\xi_3(t) \\ &+r_4^{1/2}(z(t),y(t),a(t))\xi_4(t) \\ &+r_5^{1/2}(z(t),y(t),a(t))\xi_5(t) \\ &-r_6^{1/2}(z(t),y(t),a(t))\xi_6(t), \end{aligned} \quad (21)$$

$$\begin{aligned} \frac{\mathrm{d}y(t)}{\mathrm{d}t} = r_7(z(t),y(t),a(t)) &- r_8(z(t),y(t),a(t)) \\ &-r_9(z(t),y(t),a(t)) \\ &+r_7^{1/2}(z(t),y(t),a(t))\xi_7(t) \\ &-r_8^{1/2}(z(t),y(t),a(t))\xi_8(t) \\ &-r_9^{1/2}(z(t),y(t),a(t))\xi_9(t), \end{aligned} \quad (22)$$

$$\begin{aligned} \frac{\mathrm{d}a(t)}{\mathrm{d}t} = r_{10}(z(t),y(t),a(t)) &- r_{11}(z(t),y(t),a(t)) \\ &-r_{12}(z(t),y(t),a(t)) \\ &+r_{10}^{1/2}(z(t),y(t),a(t))\xi_{10}(t) \\ &-r_{11}^{1/2}(z(t),y(t),a(t))\xi_{11}(t) \\ &-r_{12}^{1/2}(z(t),y(t),a(t))\xi_{12}(t), \end{aligned} \quad (23)$$

where $\xi_{i=1,\ldots,12}(t)$ are temporally uncorrelated, statistically independent Gaussian white noises with $\langle \xi_i(t)\rangle = 0$ and $\langle \xi_i(t)\xi_j(s)\rangle = \delta_{ij}\delta(t-s)$.

By using the relationship between the concentration and the molecular number of each species, Eq. (4), the CLE corresponding to the macroscopic differential Eqs. (1)–(3) can be obtained from Eqs. (21)–(23) and read as

$$\frac{dZ}{dt} = (V_0 + V_1\beta - V_2 + V_3 + k_f Y - kZ) + \frac{1}{\sqrt{\Omega}}\Big[\sqrt{V_0}\xi_1(t) + \sqrt{V_1\beta}\xi_2(t) - \sqrt{V_2}\xi_3(t) + \sqrt{V_3}\xi_4(t) + \sqrt{k_f Y}\xi_5(t) \quad -\sqrt{kZ}\xi_6(t)\Big], \tag{24}$$

$$\frac{dY}{dt} = (V_2 - V_3 - k_f Y) + \frac{1}{\sqrt{\Omega}}\Big[\sqrt{V_2}\xi_7(t) - \sqrt{V_3}\xi_8(t) - \sqrt{k_f Y}\xi_9(t)\Big], \tag{25}$$

$$\frac{dA}{dt} = (\beta V_4 - V_5 - \varepsilon A) + \frac{1}{\sqrt{\Omega}}\Big[\sqrt{\beta V_4}\xi_{10}(t) - \sqrt{V_5}\xi_{11}(t) - \sqrt{\varepsilon A}\xi_{12}(t)\Big]. \tag{26}$$

It can be noted that the internal fluctuation item is proportional to $1/\sqrt{\Omega}$ in the mesoscopic stochastic differential Eqs. (24) (25) (26) when the other parameters are fixed, and vanishes in the thermodynamic limit (i.e. $\Omega \to \infty$).

The model Eqs. (1)–(3) for cytosolic Ca^{2+} behaviors shows not only for simple periodic Ca^{2+} oscillations, but also for some complex oscillatory phenomena. The dynamic behavior of the model in parameter space had been investigated in Ref. [46], and it was shown that the complex Ca^{2+} oscillatory behaviors include bursting, chaos and quasi-periodicity. Four sets of parameter values corresponding to the simple oscillations and the complex oscillatory behaviors are listed in Table 4. To study the effects of the finite molecule number on both simple and complex Ca^{2+} oscillations, numerical simulations are needed, and the mesoscopic stochastic Eqs. (24)–(26) are simulated by using a simple forward Euler algorithm with a time step of 0.001 min. In each calculation the time evolution of the system lasted 1000 min after transient behavior was discarded.

Table 4
Parameter values corresponding to the simple oscillations and the various types of complex oscillatory behavior in the Ca^{2+} oscillations model [46]

Parameters	Simple oscillation	Bursting	Chaos	Quasi-periodicity
n	4.0	2.0	4.0	4.0
m	2.0	4.0	2.0	2.0
p	2.0	1.0	1.0	2.0
β	0.50	0.46	0.65	0.51
K_2 (μM)	0.1	0.1	0.1	0.1
K_5 (μM)	1.0	1.0	0.3194	0.3
K_A (μM)	0.2	0.1	0.1	0.2
K_d (μM)	0.4	0.6	1.0	0.5
K_Y (μM)	0.2	0.2	0.3	0.2
K_Z (μM)	0.5	0.3	0.6	0.5
k (min^{-1})	10.0	10.0	10.0	10.0
k_f (min^{-1})	1.0	1.0	1.0	1.0
ϵ (min^{-1})	0.1	1.0	13.0	0.1
V_0 (μM min^{-1})	2.0	2.0	2.0	2.0
V_1 (μMmin^{-1})	2.0	2.0	2.0	2.0
V_{M2} (μM min^{-1})	6.0	6.0	6.0	6.0
V_{M3} (μM min^{-1})	20.0	20.0	30.0	20.0
V_4 (μM min^{-1})	2.0	2.5	3.0	5.0
V_{M5} (μM min^{-1})	5.0	30.0	50.0	30.0

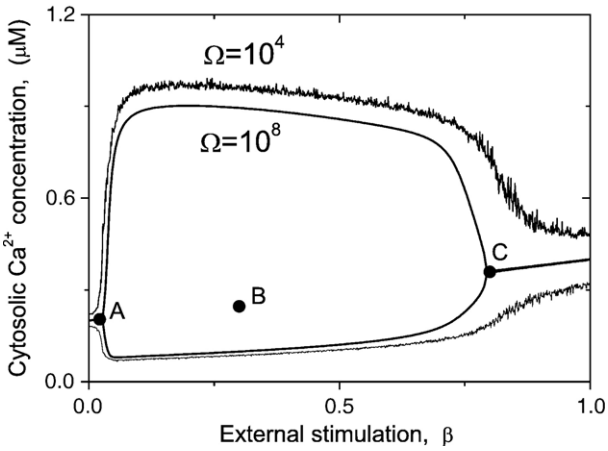

Fig. 2. Bifurcation diagram for simple intracellular calcium oscillation, where β=0.028 for point A, β=0.3 for point B, and β=0.8 for point C.

3. Effects of finite total molecule number on intracellular calcium oscillations

It is well known that Ca^{2+} relays information within cells to regulate their activity, and the information can be encoded by both the frequency and the amplitude of Ca^{2+} oscillations. In this section, the effects of total molecule number on the various types of intracellular calcium oscillations have been investigated through the power spectrum and the distribution (the histogram) of Ca^{2+} concentration.

3.1. Simple intracellular calcium oscillation

The external control parameter β has two supercritical Hopf bifurcation points for the macroscopic kinetics. The intracellular Ca^{2+} concentration is oscillated for $\beta_1 < \beta < \beta_2$, and is stable steady state for $\beta < \beta_1$ or $\beta > \beta_2$. It is known that the smaller the molecule number is, the larger the internal fluctuation will be. For the mesoscopic kinetics (i.e. Eqs. (24)–(26)), the bifurcation diagrams for different molecule numbers are plotted in Fig. 2. Three values of the external control parameter β (=0.028, 0.3, 0.8, marked by A, B and C in Fig. 2) were chosen to discuss the effects of finite molecule number on the intracellular Ca^{2+} oscillation.

When β=0.3 (at which the intracellular Ca^{2+} concentration shows simple oscillations in the case of macroscopic kinetics), the cytosolic Ca^{2+} oscillation and the histogram of Ca^{2+} concentration are plotted in Fig. 3 for different molecule numbers Ω. It is shown that there is only one peak in the histogram of Ca^{2+} concentration, which is located at low cytosolic Ca^{2+} concentration for small Ω. With the increase of molecule number, a tiny peak appeared at high Ca^{2+} concentration states.

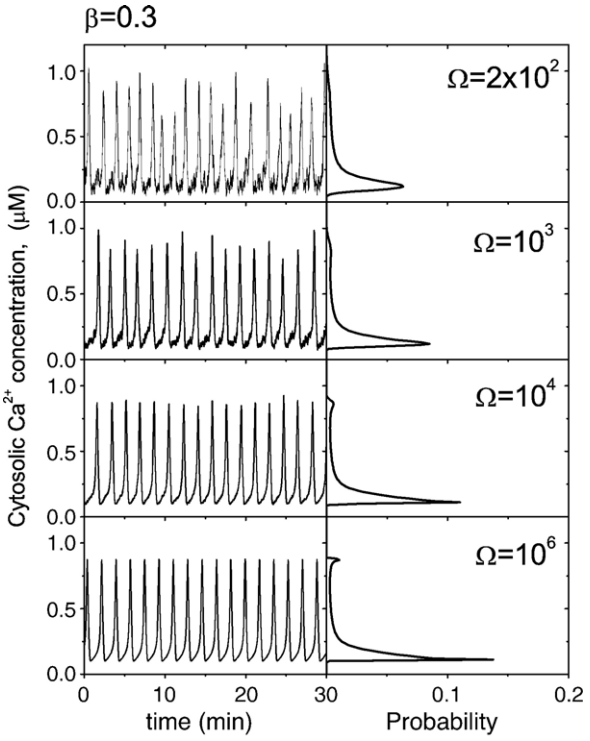

Fig. 3. Temporal evolution of cytosolic Ca^{2+} concentration (left) and corresponding histogram of Ca^{2+} concentration (right) for different molecule numbers Ω. The other parameter values corresponding to the simple cytosolic oscillation are listed in Table 4.

To characterize the effects of finite molecule number on the stochastic cytosolic Ca^{2+} oscillation, the coefficient of variation (CV) [76]

$$\mathrm{CV} = \sqrt{\frac{\langle T^2\rangle - \langle T\rangle^2}{\langle T\rangle}} \tag{27}$$

has been calculated, where $\langle T\rangle := \lim_{N\to\infty}\sum_{i=1}^{N}(t_{i+1}-t_i)/N$ and $\langle T^2\rangle := \lim_{N\to\infty}\sum_{i=1}^{N}(t_{i+1}-t_i)^2/N$ are the mean and mean-squared interspike intervals, respectively. A spike in the Ca^{2+} concentration $Z(t_i)$ occurred at time t_i. In our computations, a spike will occur when the Ca^{2+} concentration exceeds a threshold (Z_c=0.5 μM). The CV presents a measure of spike coherence (i.e. the order degree of stochastic Ca^{2+} oscillations). With the increase of Ω, Fig. 4 shows that the mean interspike interval is increased, and then tends to a limit value 1.78218 min (the period of cytosolic Ca^{2+} oscillations in the case of macroscopic kinetics), while the CV is decreased and tends to zero if $\Omega\to\infty$.

When β=0.028 or β=0.8 (at which the intracellular Ca^{2+} concentration is stable steady state in the case of macroscopic kinetics), the power spectrum of cytosolic Ca^{2+} concentration for different Ω is plotted in Fig. 5. A Welch window function is used during the estimation of power spectrum. The time series of stochastic calcium concentration Z contains 2^{16} data points, and the smoothed curves of power spectrum are obtained by nearest averaging over 50 points. It can be found that there exists a peak of power spectrum. With the increase of molecule

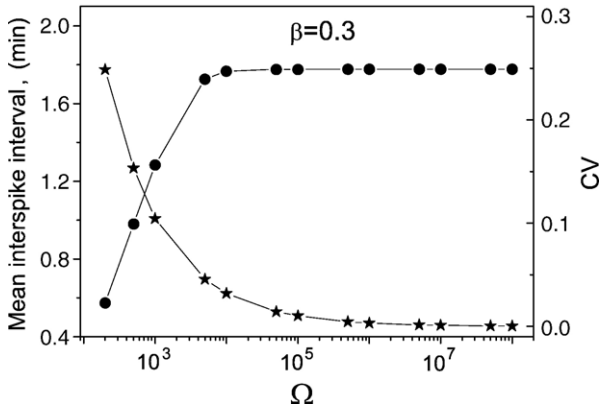

Fig. 4. Mean interspike interval $\langle T\rangle$ (dot line) and its coefficient of variation (CV) (star line) as a function of the molecule number. The other parameter values are the same as in Fig. 3.

number (in other words, with the decrease of internal fluctuation), (i) the height of power spectrum's peak is increased firstly, reaches a maximum, and then is decreased; (ii) the width of power spectrum's peak becomes narrower; (iii) our computation results also showed that the optimal frequency corresponding to the peak shifts from low to high when the molecule number is increased from 10^2 to 10^5, however, the optimal frequency is nearly not varied when $\Omega > 10^5$.

The above results show that there exists the most pronounced peak of power spectrum for certain intermediate molecule number. To quantify the relative performance of the stochastic calcium concentration oscillations, one can define an effective SNR [60–62,71–74,76]:

$$\mathrm{SNR} = R\frac{\omega_p}{\Delta\omega}, \tag{28}$$

where ω_p is the frequency at the peak, $\Delta\omega$ is the width between ω_p and ω_1 satisfying $\omega_1 > \omega_p$ and $P(\omega_1)=P(\omega_p)/e$, $R=P(\omega_p)/P(\omega_2)$, and $P(\omega_2)$ is the smallest power spectrum value ($0<\omega_2<\omega_p$). The SNR with the increase of molecule number is

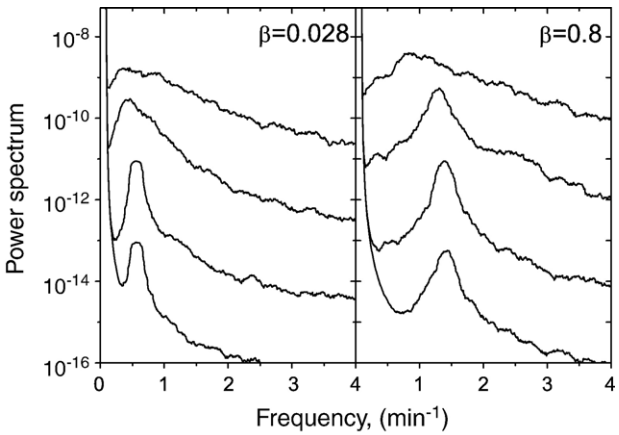

Fig. 5. Power spectrum of cytosolic Ca^{2+} concentration for β=0.028 (left) and β=0.8 (right). From top to bottom: $\Omega=10^2$, 10^4, 10^6, and 10^8. The other parameter values are the same as in Fig. 3.

respectively plotted for $\beta=0.028$ and $\beta=0.8$ in Fig. 6. It is clear that there is a maximum of SNR at certain optimal molecule numbers ($\Omega\sim10^6$ under the given values of β here). This is a signature of resonance which is the typical coherence resonance or autonomous resonance phenomenon since there is no external periodic signal. It should be pointed out that (i) the maximum of SNR and the coherence resonance had been found by Meinhold and Schimansky-Geier [60] corresponding to the optimal IP_3R-I channel numbers of a single cluster there, but corresponding to the optimal biochemical reaction molecule numbers here. (ii) It was also found that [77,78] the optimal system size (i.e. the volume) of SNR depends on the external control parameter, the optimal volume matches well with the real cell volume when the control parameter is tuned near the left Hopf bifurcation point, and the size of real living cells in vivo is around 10^3 μm^3 [68].

3.2. Complex intracellular calcium oscillation

Complex Ca^{2+} oscillatory behaviors of the model include bursting, chaos and quasi-periodicity. In the case of mesoscopic kinetics of intracellular Ca^{2+} oscillations, the time series of cytosolic Ca^{2+} concentration for the three types of complex Ca^{2+} oscillations is plotted in Fig. 7, respectively. When the molecule number Ω is small (e.g. $\Omega=200$), various Ca^{2+} oscillatory types are hard to distinguish, and the irregularity of the oscillations shows up both in the amplitude and in the time interval between successive Ca^{2+} spikes due to the large internal fluctuation. However, with the increase of molecule number (or decrease of the intrinsic fluctuation), the differences between various cytosolic Ca^{2+} oscillation types of complex Ca^{2+} oscillations are much more remarkable.

To characterize the effects of finite molecule number on the complex cytosolic Ca^{2+} oscillations, the histograms of Ca^{2+} concentration for different molecule numbers Ω are shown in Fig. 8. For the bursting type, when the molecule number is very small (e.g. $\Omega=200$), there is only one peak located at low Ca^{2+} concentration state in the histograms of Ca^{2+} concentration. With the increase of molecule number, more and more peaks appeared at moderate Ca^{2+} concentration states, and a tiny peak at highest concentration state also existed. For the chaos type, when $10^3<\Omega<5\times10^5$, there are visibly two peaks in the histograms of Ca^{2+} concentration; it can be seen that the height of peak at low concentration is higher than that at high concentration first (e.g. $\Omega=10^3$); with the increase of molecule

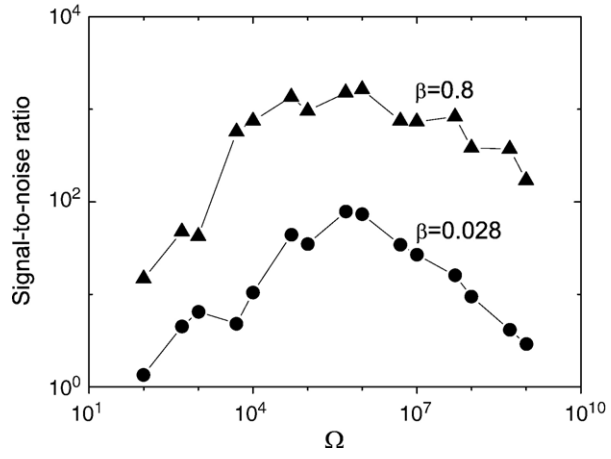

Fig. 6. Signal-to-noise ratio vs. the finite molecule number for $\beta=0.028$ and $\beta=0.8$. The other parameter values are the same as in Fig. 3.

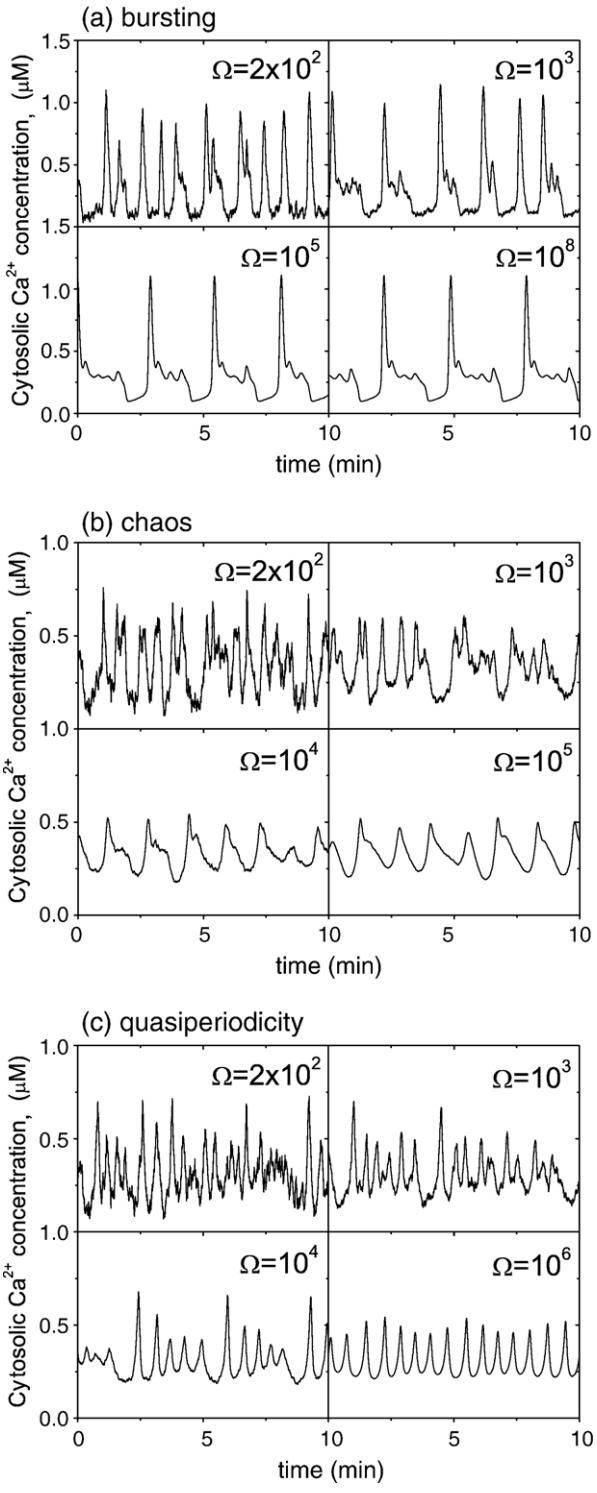

Fig. 7. Temporal evolution of three cytosolic Ca^{2+} oscillatory types for different molecule numbers Ω. The other parameter values corresponding to three oscillatory types are listed in Table 4.

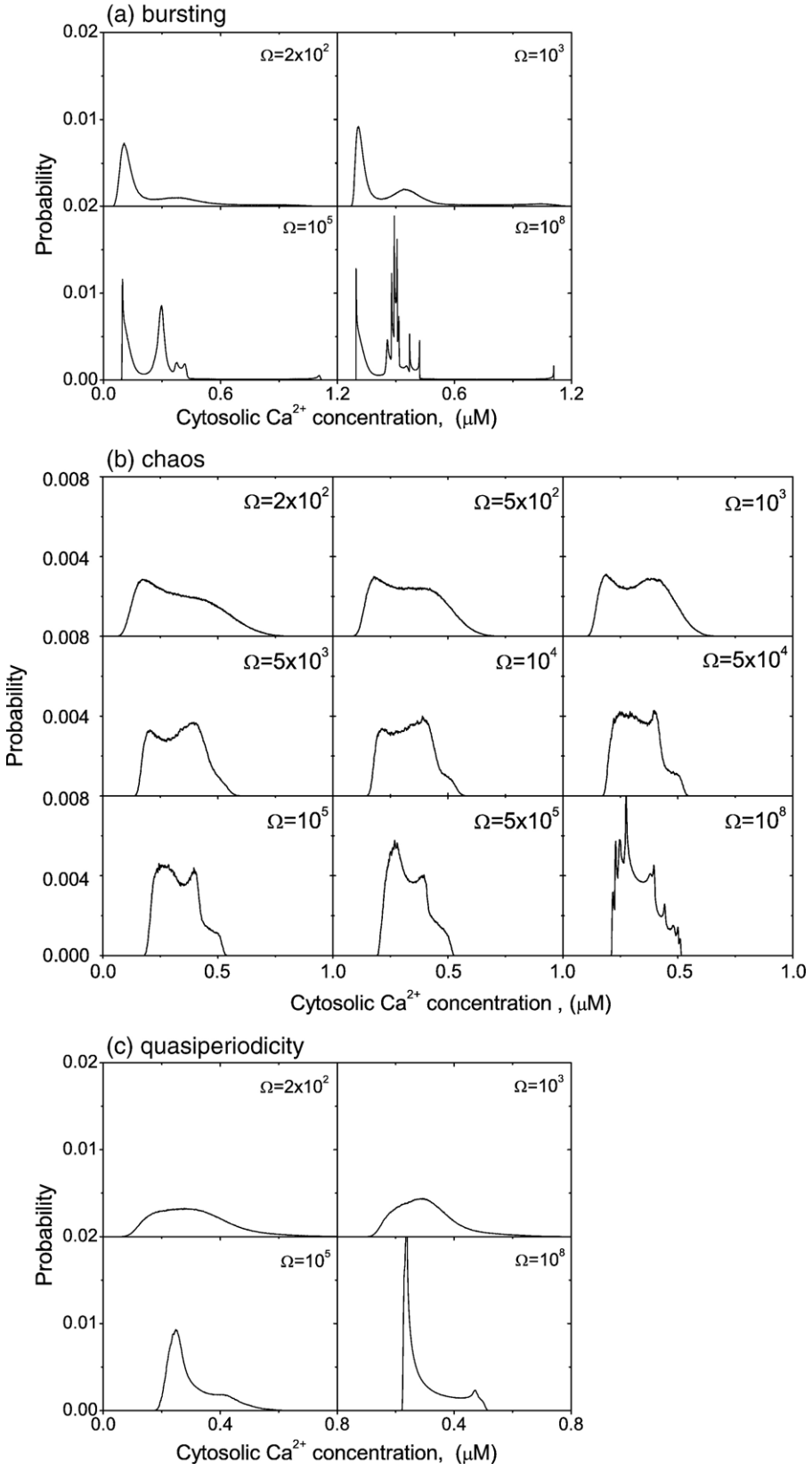

Fig. 8. Histograms of complex cytosolic Ca^{2+} concentration for different molecule numbers Ω. The bin-size is 0.001 μM. The other parameter values corresponding to various complex cytosolic Ca^{2+} oscillatory types are listed in Table 4.

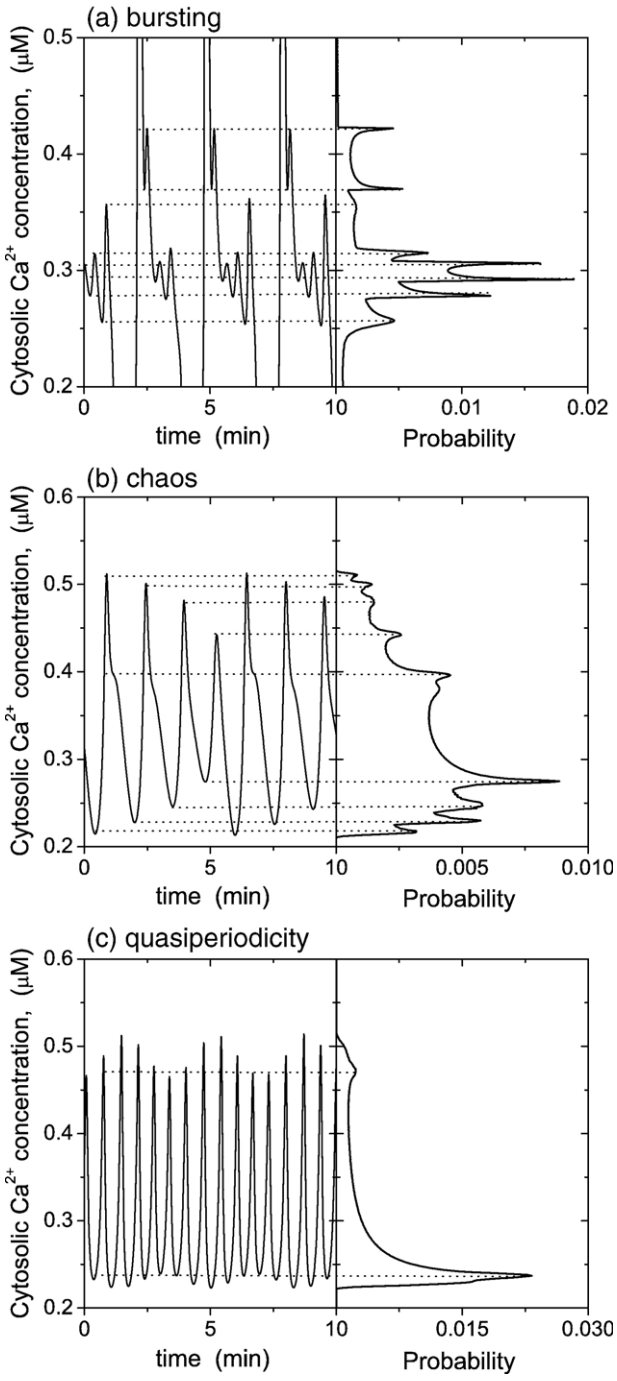

Fig. 9. Temporal evolution of cytosolic Ca^{2+} concentration (left) and corresponding histogram of Ca^{2+} concentration amplitude (right) when $\Omega=10^8$. The other parameter values corresponding to various oscillatory types are listed in Table 4.

number, the height of peak at low concentration becomes lower than that at high concentration (e.g. $\Omega=5\times10^3$); when the molecule number is continuously increased, however, the height of peak at low concentration is higher than that at high concentration again (e.g. $\Omega=5\times10^5$). For the quasi-periodicity type, there is only one peak located at low Ca^{2+} concentration in the histograms of amplitude of cytosolic Ca^{2+} concentration for different molecule numbers, and only a tiny peak appeared at high Ca^{2+} concentration when the molecule number is very large (e.g. $\Omega=10^8$).

The above results also show that, when the molecule number Ω becomes large, the property of the histogram of cytosolic Ca^{2+} concentration for various complex Ca^{2+} oscillatory types is different. Fig. 9 shows the time series of the three Ca^{2+} oscillatory types and the corresponding histogram of Ca^{2+} concentration for $\Omega=10^8$. For the bursting and chaos types, it

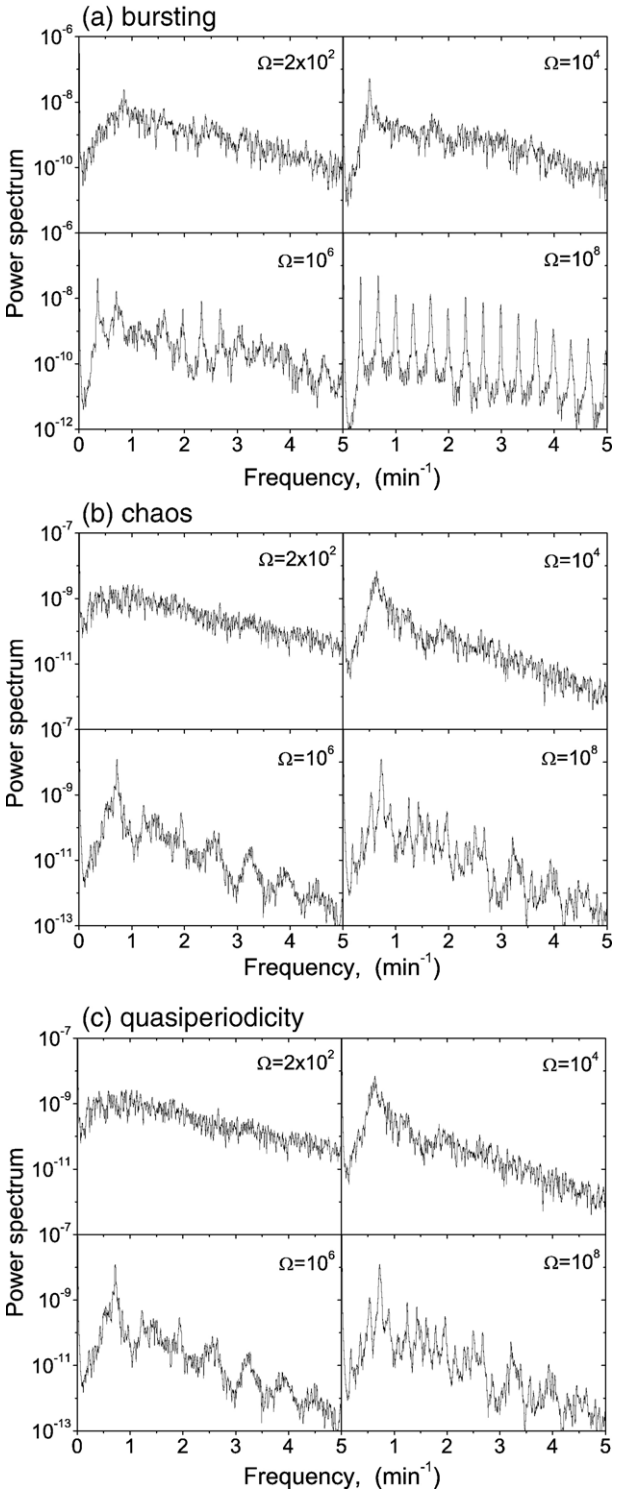

Fig. 10. Power spectrum of various complex cytosolic Ca^{2+} oscillatory types for different molecule numbers Ω. The other parameter values corresponding to three complex Ca^{2+} oscillations are listed in Table 4.

is found that each extremum (including maximum and minimum) of concentration of cytosolic Ca^{2+} oscillations corresponds to a peak in the histogram of Ca^{2+} concentration, and the most probability appeared during the bursting plateau level (i.e. $Z=0.292$ μM) for the bursting type, while it is at the largest minimum of Ca^{2+} concentration (i.e. $Z=0.275$ μM) for the chaos type. For the quasi-periodicity type, however, there are only two peaks (located at low Ca^{2+} concentration and high Ca^{2+} concentration, respectively) in the histogram of Ca^{2+} concentration, and the most probability is around the minimum of cytosolic Ca^{2+} concentration (i.e. $Z=0.237$ μM).

The power spectra of various complex cytosolic Ca^{2+} oscillatory types for different Ω are plotted in Fig. 10. A Welch window function is used during the estimation of power spectrum. The time series of stochastic cytosolic calcium concentration Z contains 2^{16} data points, and the smoothed curves of power spectrum are obtained by nearest averaging over 5 points. When the molecule number is very small (e.g. $\Omega=2\times10^2$), or the intrinsic fluctuation of the system is very large, high irregularity of the intracellular Ca^{2+} oscillations shows up both in the amplitude and in the time interval between successive Ca^{2+} spikes for various Ca^{2+} oscillatory types (see Fig. 7), and the three oscillatory types are hard to distinguish. On the other hand, Fig. 10 shows that there is a peak of power spectrum for various types of complex oscillations for $\Omega=2\times10^2$; the frequency corresponding to the maximum of power spectrum is called as the optimal frequency of cytosolic Ca^{2+} stochastic oscillations. With the increase of molecule number, the optimal frequency is shifted from high frequency to low one, meanwhile, the natural frequencies of system (all the frequencies discussed here are multiples of the smallest natural frequency, e.g. $\Omega=10^8$) become distinguishable for bursting; the frequency corresponding to the unstable limit cycle in the case of macroscopic kinetics [46] becomes discernible for both chaos and quasi-periodicity.

4. Conclusions

Based on the model of intracellular Ca^{2+} oscillation with self-modulation of IP_3 signal [46] to describe both simple and complex intracellular calcium oscillations, the mesoscopic stochastic differential equations for the intracellular Ca^{2+} oscillation have been derived by using the Gillespie's method (or the chemical Langevin equation) [75] in this paper, which provide us with a convenient mathematical method to study the intrinsic fluctuation in cellular or subcellular level. It should be stressed that the mesoscopic stochastic kinetics for the intracellular Ca^{2+} oscillations is valid only under two conditions being satisfied, one is the macroscopically infinitesimal time increment must be of short enough duration that the propensity of each reaction term does not change significantly during the macroscopically infinitesimal time increment, the other is the macroscopically infinitesimal time increment must be of long enough duration that each reaction channel fires several times during the macroscopically infinitesimal time increment.

The effects of the finite biochemical reaction molecule number on both simple and complex cytosolic Ca^{2+} oscillations have been theoretically studied through numerical computation, respectively. In the case of simple intracellular Ca^{2+} oscillation, with the increase of molecule number, it is found that the coherence resonance or autonomous resonance phenomena can occur for some external stimulation parameter values. In the cases of complex intracellular Ca^{2+} oscillations, the histograms of Ca^{2+} oscillations are different for each typical complex Ca^{2+} oscillatory behavior in finite biochemical reaction molecule number.

The physiological information can be encoded by both the frequency and the amplitude of cytosolic Ca^{2+} oscillations; the above results might be helpful to understand how the intrinsic fluctuation due to the finite biochemical reaction molecule number in live cell affect the cytosolic Ca^{2+} relaying of the information within cells to regulate their activity. The above results about the effects of finite biochemical reaction molecule number on cytosolic Ca^{2+} oscillations are obtained at given external control parameter, that is, the extracellular stimulation is a constant. However, in a live cell system, the random extracellular agonists such as hormones and neurotransmitters are unavoidable. Therefore, we expect that more novel physical and richer physiological phenomena in the cellular and subcellular level could be observed when the random extracellular stimulations or the external fluctuations are considered, and this is our further work.

Acknowledgments

The authors are very grateful to the two anonymous referees for their valuable comments and suggestions. This work was supported by the National Natural Science Foundation of China under Grant No. 10575041 and partly supported by MOE of China under Grant No. SRFDP-20040511005.

References

[1] P. Cohen, A. Burchell, J.G. Foulkes, P.T.W. Cohen, T.C. Vanaman, A.C. Nairn, Identification of the Ca^{2+}-dependent modulator protein as the fourth subunit of rabbit skeletal muscle phosphorylase kinase, FEBS Lett. 92 (1978) 287–293.

[2] K. Morita, K. Koketsu, K. Kuba, Oscillation of $[Ca^{2+}]_i$-linked K^+ conductance in bullfrog sympathetic ganglion cell is sensitive to intracellular anions, Nature 283 (1980) 204–205.

[3] A. Goldbeter, D.E. Koshland, An amplified sensitivity arising from covalent modification in biological systems, Proc. Natl. Acad. Sci. U. S. A. 78 (1981) 6840–6844.

[4] K.S.R. Cuthbertson, P.H. Cobbold, Phorbol ester and sperm activate mouse oocytes by inducing sustained oscillations in cell Ca^{2+}, Nature 316 (1985) 541–542.

[5] N.M. Wood, K.S.R. Cuthbertson, P.H. Cobbold, Repetitive transient rises in cytoplasmic free calcium in hormone-stimulated hepatocytes, Nature 319 (1986) 600–602.

[6] N.M. Wood, K.S.R. Cuthbertson, P.H. Cobbold, Agonist-induced oscillations in cytoplasmic free calcium concentration in single rat hepatocytes, Cell Calcium 8 (1987) 79–100.

[7] T.A. Rooney, E.J. Sass, A.P. Thomas, Agonist-induced cytosolic calcium oscillations originate from a specific locus in single hepatocytes, J. Biol. Chem. 265 (1990) 10792–10796.

[8] M. Craske, T. Takeo, O. Gerisamenko, C. Vaillant, K. Torok, O. Petersen, A. Tepikin, Hormone-induced secretory and nuclear translocation of calmodulin: oscillations of calmodulin concentration with the nucleus as integrator, Proc. Natl. Acad. Sci. U. S. A. 96 (1990) 4426–4431.

[9] M.J. Berridge, Inositol trisphosphate and calcium signalling, Nature 361 (1993) 315–325.
[10] A.K. Green, C.J. Dixon, A.G. MacLennan, P.H. Cobbold, M.J. Fisher, Adenine dinucleotide-mediated cytosolic free Ca^{2+} oscillations in single hepatocytes, FEBS Lett. 322 (1993) 197–200.
[11] M.R. McAinsh, A.A.R. Wegg, J.E. Taylor, A.M. Hetherington, Stimulus-induced oscillations in guard-cell cytosolic free calcium, Plant Cell 7 (1995) 1207–1219.
[12] A. Goldbeter, Biochemical oscillations and cellular rhythms. The molecular bases of periodic and chaotic behaviour, Cambridge University Press, Cambridge, 1996.
[13] M.J. Beridge, M.D. Bootman, P. Lipp, Calcium—a life and death signal, Nature 395 (1998) 645–648.
[14] K.T. Jones, Ca^{2+} oscillations in the activation of the egg and development of the embryo in mammals, Int. J. Dev. Biol. 42 (1998) 1–10.
[15] B. Soria, F. Martin, Cytosolic calcium oscillations and insulin release in pancreatic islets of Langerhans, Diabetes Metab. (Pairs) 24 (1998) 37–40.
[16] P. De Koninck, H. Schulman, Sensitivity of CaM kinase II to the frequency of Ca^{2+} oscillations, Science 279 (1998) 227–230.
[17] R.E. Dolmetsch, K. Xu, R. Lewis, Calcium oscillations increase the efficiency and specificity of gene expression, Nature 392 (1998) 933–936.
[18] W.H. Li, J. Llopis, M. Whitney, G. Zlokarnlk, R.Y. Tsien, Cell-permeant caged $InsP_3$ ester shows that Ca^{2+} spike frequency can optimize gene expression, Nature 392 (1998) 936–941.
[19] M. Marhl, S. Schuster, M. Brumen, Mitochondria as an import factor in the maintenance of constant amplitudes of cytosolic calcium oscillations, Biophys. Chem. 71 (1998) 125–132.
[20] K.U. Bayer, P. De Koninck, S. Schulman, Alternative splicing modulate the frequency-dependent response of CaMKII to Ca^{2+} oscillations, EMBO J. 21 (2002) 3590–3597.
[21] C. Schofl, G. Brabant, R.D. Hesch, A. von zur Muhlen, P.H. Cobbold, K.S.R. Cuthbertson, Temporal patterns of α_1-receptor stimulation regulate amplitude and frequency of calcium transients, Am. J. Physiol. 265 (1993) C1030–C1036.
[22] R.E. Dolmetsch, R.S. Lewis, C.C. Goodnow, J.I. Healy, Differential activation of transcription factors induced by Ca^{2+} response amplitude and duration, Nature 386 (1997) 855–858.
[23] K. Prank, F. Gabbiani, G. Brabant, Coding efficiency and information rates in transmembrane signaling, Biosystems 55 (2000) 15–22.
[24] S. Schuster, M. Narhl, T. Höfer, Modelling of simple and complex calcium oscillations from single-cell responses to intercellular signalling, Eur. J. Biochem. 269 (2002) 1333–1355.
[25] M. Falcke, Reading the patterns in living cells—the physics of Ca^{2+} signaling, Adv. Phys. 53 (2004) 255–440.
[26] T. Meyer, L. Stryer, Molecular model for receptor-stimulated calcium spiking, Proc. Natl. Acad. Sci. U. S. A. 85 (1988) 5051–5055.
[27] T. Meyer, L. Stryer, Calcium spiking, Ann. Rev. Biophys. Chem. 20 (1991) 153–174.
[28] A. Goldbeter, G. Dupont, M.J. Berridge, Minimal model for signal-induced Ca^{2+} oscillations and for their frequency encoding through protein phosphorylation, Proc. Natl. Acad. Sci. U. S. A. 87 (1990) 1461–1465.
[29] K.S.R. Cuthbertson, T.R. Chay, Modelling receptor-controlled intracellular calcium oscillations, Cell Calcium 12 (1991) 97–109.
[30] R. Somogyi, J.W. Stucki, Hormone-induced calcium oscillations in liver cells can be explained by a simple one pool model, J. Biol. Chem. 266 (1991) 11068–11077.
[31] G.W. De Young, J. Keizer, A single-pool inositol 1,4,5-trisphosphate-receptor-based model for agonist-stimulated oscillations in Ca^{2+} concentration, Proc. Natl. Acad. Sci. U. S. A. 89 (1992) 9895–9899.
[32] G. Dupont, A. Goldbeter, Protein phosphorylation driven by intracellular calcium oscillations: a kinetic analysis, Biophys. Chem. 42 (1992) 257–270.
[33] G. Dupont, A. Goldbeter, One-pool model for Ca^{2+} oscillations involving Ca^{2+} and inositol 1,4,5-trisphosphate as co-agonists for Ca^{2+} release, Cell Calcium 14 (1993) 311–322.
[34] Y.X. Li, J. Rinzel, J. Keizer, S.S. Stojilkovic, Calcium oscillations in pituitary gonadotrophs: comparison of experiment and theory, Proc. Natl. Acad. Sci. U. S. A. 91 (1994) 58–62.
[35] Y.X. Li, J. Rinzel, Equations for $InsP_3$ receptor-mediated $[Ca^{2+}]_i$ oscillations derived from a detailed kinetic model: a Hodgkin-Huxley like formalism, J. Theor. Biol. 166 (1994) 461–473.
[36] I. Marrero, A. Sanchez-Bbueno, P.H. Cobbold, C.J. Dixon, Taurolitocholate and taurolitocholate 3-sulfate exert different effects on cytosolic free Ca^{2+} concentration in rat hepatocytes, Biochem. J. 300 (1994) 383–386.
[37] T. Chay, Y.S. Fan, Y.S. Lee, Bursting, spiking, chaos, fractals, and universality in biological rhythms, Int. J. Bifurc. Chaos Appl. Sci. Eng. 5 (1995) 595–635.
[38] P. Shen, R. Larter, Chaos in intracellular Ca^{2+} oscillations in a new model for non-excitable cells, Cell Calcium 17 (1995) 225–232.
[39] T.R. Chay, Electrical bursting and luminal calcium oscillation in excitable cell models, Biol. Cybern. 75 (1996) 419–431.
[40] M.L. Cárdenas, A. Goldbeter, The glucose induced switch between glycogen phosphorylase and glycogen synthase in the liver: outlines of theoretical approach, J. Theor. Biol. 182 (1996) 421–426.
[41] J.A.M. Borghans, G. Dupont, A. Goldbeter, Complex intracellular calcium oscillations, a theoretical exploration of possible mechanism, Biophys. Chem. 66 (1997) 25–41.
[42] M. Marhl, S. Schuster, M. Brumen, R. Heinrich, Modelling the interrelations between calcium oscillations and ER membrane potential oscillations, Biophys. Chem. 63 (1997) 221–239.
[43] M. Marhl, S. Schuster, M. Brumen, R. Heinrich, Complex calcium oscillations and the role of mitochondria and cytosolic proteins, Biosystems 57 (2000) 75–86.
[44] S. Schuster, M. Marhl, Bifurcation analysis of calcium oscillations: time-scale separation, canards, and frequency lowering, J. Biol. Syst. 9 (2001) 291–314.
[45] M. Bollen, S. Keppens, W. Stalmans, Specific features of glycogen metabolism in the liver, Biochem. J. 336 (1998) 19–31.
[46] G. Houart, G. Dupont, A. Gldbeter, Bursting, chaos and birhythmicity originating from self-modulation of the inositol 1,4,5-trisphosphate signal in a model for intracellular Ca^{2+} oscillations, Bull. Math. Biol. 61 (1999) 507–530.
[47] T. Tordjmann, B. Berthon, M. Claret, L. Combettes, Coordinated intercellular calcium waves induced by noradrenaline in rat hepatocytes: dual control by gap junction permeability and agonist, EMBO J. 16 (1997) 5398–5407.
[48] T. Tordjmann, B. Berthon, E. Jacquemin, C. Clair, N. Stelly, G. Guillon, M. Claret, L. Combettes, Receptor-oriented intercellular waves evoked by vasopressin in rat hepatocytes, EMBO J. 17 (1998) 4695–4703.
[49] G. Dupont, T. Tordjmann, C. Clair, S. Swillens, M. Claret, L. Combettes, Mechanism of receptor-oriented intercellular calcium wave propagation in hepatocytes, FASEB J. 14 (2000) 279–289.
[50] Höfer, Model of intercellular calcium oscillations in hepatocytes: synchronization of heterogeneous cells, Biophys. J. 77 (1999) 1244–1256.
[51] Höfer, A. Politi, R. Heinrich, Intercellular Ca^{2+} wave propagation through gap-junctional Ca^{2+} diffusion: a theoretical study, Biophys. J. 80 (2001) 75–87.
[52] J. Sneyd, M. Falcke, Models of the inositol trisphosphate receptor, Prog. Biophys. Mol. Biol. 89 (2005) 207–245.
[53] D. Gall, E. Baus, G. Dupont, Activation of the liver glycogen phosphorylase by Ca^{2+} oscillations: a theoretical study, J. Theor. Biol. 207 (2000) 445–454.
[54] U. Kummer, L.F. Olsen, C.J. Dixon, A.K. Green, E. Bornberg-Bauer, G. Baier, Switching from simple to complex oscillations in calcium signaling, Biophys. J. 79 (2000) 1188–1195.
[55] T. Haberichter, M. Marhl, R. Heinrich, Birhythmicity, trirhythmicity and chaos in bursting calcium oscillations, Biophys. Chem. 90 (2001) 17–30.
[56] Y. Jia, L.J. Yang, D. Wu, Q. Liu, X. Zhan, Noise-induced bursting and coherence resonance in minimal cytosolic Ca^{2+} oscillation model, Chin. Phys. Lett. 21 (2004) 1666–1669.
[57] S. Swillens, P. Champeil, L. Combettes, G. Dupont, Stochastic simulation of a single inositol 1,4,5-trisphosphate-sensitive Ca^{2+}-channel reveals repetitive openings during blip-like Ca^{2+} transients, Cell Calcium 23 (1998) 291–302.

[58] M. Falcke, On the role of stochastic channel behavior in intracellular Ca^{2+} dynamics, Biophys. J. 84 (2003) 42–56.
[59] M. Falcke, M. Or-Guil, M. Bär, Dispersion gap and localized spiral waves in a model for intracellular Ca^{2+} dynamics, Phys. Rev. Lett. 84 (2000) 4753–4756.
[60] L. Meinhold, L. Schimansky-Geier, Analytic description of stochastic calcium-signaling periodicity, Phys. Rev., E Stat. Phys. Plasmas Fluids Relat. Interdiscip. Topics 66 (2002) 050901 (R)-1-4.
[61] J.W. Shuai, P. Jung, Optimal ion channel clustering for intracellular calcium signaling, Proc. Natl. Acad. Sci. U. S. A. 100 (2003) 506–510.
[62] J.W. Shuai, P. Jung, Optimal intracellular calcium signaling, Phys. Rev. Lett. 88 (2002) 068102-1-4.
[63] R. Thul, M. Falcke, Release currents of IP_3 receptor channel clusters and concentration profiles, Biophys. J. 86 (2004) 2660–2673.
[64] S. Swillens, G. Dupont, L. Combettes, P. Champeil, From calcium blips to calcium puffs: theoretical analysis of the requirements for interchannel communication, Proc. Natl. Acad. Sci. U. S. A. 96 (1999) 13750–13755.
[65] A. Sherman, J. Rinzel, J. Keizer, Emergence of organized bursting in clusters of pancreatic β-cells by channel sharing, Biophys. J. 54 (1988) 411–425.
[66] M. Bär, M. Falcke, H. Levine, L. Tsimring, Discrete stochastic modeling of calcium channel dynamics, Phys. Rev. Lett. 84 (2000) 5664–5667.
[67] M. Falcke, L. Tsimring, H. Levine, Stochastic spreading of intracellular Ca^{2+} release, Phys. Rev., E Stat. Phys. Plasmas Fluids Relat. Interdiscip. Topics 62 (2000) 2636–2643.
[68] M.E. Grachva, R. Toral, J.D. Gunton, stochastic effects in intercellular calcium spiking in hepatocytes, J. Theor. Biol. 212 (2001) 111–125.
[69] M. Kraus, P. Lais, B. Wolf, Structured biological modelling: a method for the analysis and simulation of biological systems applied to oscillatory intracellular calcium waves, Biosystems 27 (1992) 145–169.
[70] M. Kraus, B. Wolf, B. Wolf, Crosstalk between cellular morphology and calcium oscillation patterns—insights from a stochastic computer model, Cell Calcium 19 (1996) 461–472.
[71] Z.H. Hou, H.W. Xin, Internal noise stochastic resonance in a circadian clock system, J. Chem. Phys. 119 (2003) 11508–11512.
[72] Z.H. Hou, H.W. Xin, Optimal system size for mesoscopic chemical oscillation, Chem. Phys. Chem. 5 (2004) 407–410.
[73] M. Yi, Y. Jia, Light noise-induced supra-threshold circadian oscillations and coherence resonance in Drosophila, Phys. Rev., E Stat. Phys. Plasmas Fluids Relat. Interdiscip. Topics 72 (2005) 012902-1-4.
[74] M. Yi, Y. Jia, Q. Liu, J.R. Li, C.L. Zhu, Enhancement of internal noise coherence resonance by modulation of external noise in a circadian oscillator, Phys. Rev., E Stat. Phys. Plasmas Fluids Relat. Interdiscip. Topics 73 (2006) 041923-1-8.
[75] D.T. Gillespie, The chemical Langevin equation, J. Chem. Phys. 113 (2000) 297–306.
[76] A.S. Pikovsky, J. Kurths, Coherence resonance in a noise-driven excitable system, Phys. Rev. Lett. 78 (1997) 775–778.
[77] H.Y. Li, Z.H. Hou, H.W. Xin, Internal noise stochastic resonance for intracellular calcium oscillations in a cell system, Phys. Rev., E Stat. Phys. Plasmas Fluids Relat. Interdiscip. Topics 71 (2005) 061916-1-6.
[78] H.Y. Li, Z.H. Hou, H.W. Xin, Internal noise enhanced detection of hormonal signal through intracellular calcium oscillations, Chem. Phys. Lett. 402 (2005) 444–449.